JACS
JOURNAL OF THE AMERICAN CHEMICAL SOCIETY
Communication
pubs.acs.org/JACS

# Current−Voltage Characteristics and Transition Voltage Spectroscopy of Individual Redox Proteins

Juan M. Artés,[†] Montserrat López-Martínez,[†] Arnaud Giraudet,[†,⊥] Ismael Díez-Pérez,[†,‡] Fausto Sanz,[†,‡,§] and Pau Gorostiza*[,†,§,∥]

[†]Institute for Bioengineering of Catalonia (IBEC), Baldiri Reixac 15-21, 08028 Barcelona, Spain
[‡]Physical Chemistry Department, University of Barcelona (UB), Martí i Franquès 1-11, Barcelona 08028, Spain
[§]Networking Research Center on Bioengineering, Biomaterials and Nanomedicine (CIBER-BBN), 50018 Zaragoza, Spain
[∥]Catalan Institution for Research and Advanced Studies (ICREA), 08010 Barcelona, Spain

Supporting Information

**ABSTRACT:** Understanding how molecular conductance depends on voltage is essential for characterizing molecular electronics devices. We reproducibly measured current−voltage characteristics of individual redox-active proteins by scanning tunneling microscopy under potentiostatic control in both tunneling and wired configurations. From these results, transition voltage spectroscopy (TVS) data for individual redox molecules can be calculated and analyzed statistically, adding a new dimension to conductance measurements. The transition voltage (TV) is discussed in terms of the two-step electron transfer (ET) mechanism. Azurin displays the lowest TV measured to date (0.4 V), consistent with the previously reported distance decay factor. This low TV may be advantageous for fabricating and operating molecular electronic devices for different applications. Our measurements show that TVS is a helpful tool for single-molecule ET measurements and suggest a mechanism for gating of ET between partner redox proteins.

Current−bias voltage ($I-V$) measurements on individual redox proteins under potentiostatic control are reported for the first time, together with the observation of a transition voltage (TV) that is related to the tunneling barriers of the electron transfer (ET) process.

ET in proteins is a fundamental process in respiratory chains and photosynthetic complexes[1] and also has important technological applications in the construction of redox sensors[2] and molecular bioelectronic devices such as memories[3] and logic gates.[4,5] The measurement of $I-V$ plots is essential for electrical characterization of devices, and in redox proteins, several techniques and configurations have been used to that end, ranging from protein monolayers[6] and conductive force microscopy in air[7] to electrochemical scanning tunneling microscopy (ECSTM).[8,9] Recent studies have reported the conductance of redox proteins wired between electrodes at fixed bias using an STM break-junction approach,[10,11] but to date, the $I-V$ characteristics of single redox proteins have never been measured under bipotentiostatic control.

An important advance in the electronic characterization of organic molecules has been the use of transition voltage spectroscopy (TVS), which has been applied to organic monolayers[12,13] as well as individual nonredox molecules.[14] The TV obtained with these measurements is related to the alignment between the energy levels in the molecule and the Fermi level of the electrodes.[14−17] The TV depends on the coupling with the electrodes (binding chemistry and contact geometry in molecular junctions) and thus is related to the junction conductance.[14]

Beyond the methodological advantages of TVS for studying electron transport and molecular contacts at the single-molecule level, the voltage dependence of molecular conductance is especially relevant for understanding the mechanism of ET in redox-active molecules, particularly in redox proteins that exchange electrons with partner proteins in the biological context. Here we used ECSTM to measure the $I-V$ characteristics of the redox protein azurin covalently bound to a Au(111) substrate (with the partner-interacting surface facing up) in 50 mM ammonium acetate buffer (pH 4.5). The experiments were carried out in an electrochemical cell under bipotentiostatic control of the probe and sample electrodes versus a Ag/AgCl (SSC) reference electrode (Figure 1a) on reduced [sample potential ($U_S$) = −0.3 V, initial probe potential ($U_P$) = 0.5 V] or oxidized azurin ($U_S$ = 0.2 V, initial $U_P$ = −0.4 V). $I-V$ measurements were carried out in either the tunneling configuration[18] (where there is no physical contact between the STM probe and the protein) or the wired configuration[10,19] [where the probe is in contact with the protein; see the discussion below and in the Supporting Information (SI)]. We initially focused on measurements in the tunneling configuration. The sample was imaged, and the probe was positioned over a region with a high protein surface concentration (Figure S1 in the SI). The probe scan was stopped at a current set point of 0.5 nA, and the STM feedback was briefly turned off during the application of a 0.5 V symmetric ramp to $U_P$ (other experimental details are provided in the SI). A two-dimensional (2D) histogram of 50 such $I-V$ curves for reduced azurin (Figure 1c) displayed two distinct behaviors, one relatively linear and the other more rectifying. The latter was not present in $I-V$ experiments on bare Au(111) (Figure S2) and is thus attributed to azurin. Individual $I-V$ curves were pooled and averaged

**Received:** August 12, 2012
**Published:** November 28, 2012

   dx.doi.org/10.1021/ja3080242 | J. Am. Chem. Soc. 2012, 134, 20218−20221

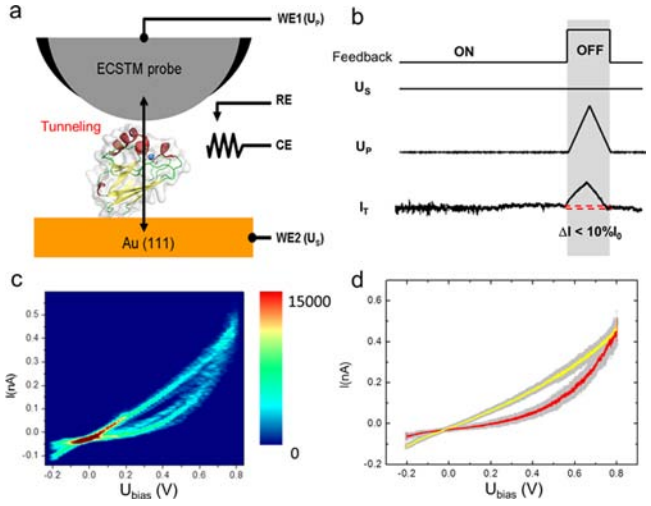


**Figure 1.** (a) Experimental setup. The azurin structure (PDB entry 1jzf[20]) is represented as a cartoon with the Cu ion shown in blue and the solvent-accessible surface in transparent gray. Abbreviations: WE, working electrode; RE, reference electrode; CE, counter electrode. (b) Example of $I-V$ recording. A triangular ramp was applied to the probe (WE1, $U_P$) while the feedback loop was off. The current signal ($I_T$) was recorded at constant sample potential (WE2, $U_S$). (c) 2D $I-V$ histogram showing two populations of curves in a sample of azurin on Au(111). Parameters: $U_S = -0.3$ V (reduced azurin); initial $U_P = 0.5$ V; current set point = 0.5 nA; $N = 50$ measurements. (d) Averages of the two $I-V$ populations identified in (c), corresponding to azurin (red) and Au (yellow). Gray error bars indicate standard deviations.

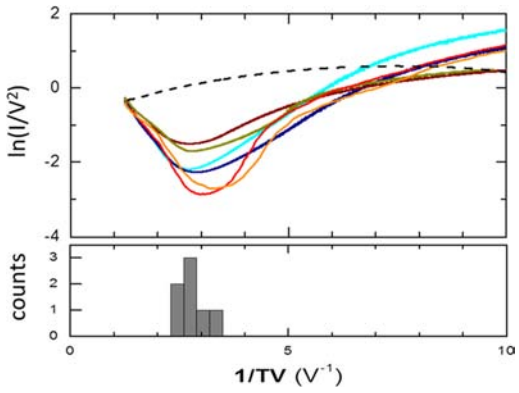


**Figure 2.** (a) TVS representation of smoothed raw-data $I-V$ curves of azurin for $U_S = -0.3$ V and initial $U_P = 0.5$ V. The dashed line shows the average $I-V$ curve for the Au control. The TV is the voltage where the plot displays a minimum. (b) Histogram showing the distribution of the minima of the plots in (a), which is centered at 0.37 ± 0.03 V.

according to this criterion and are presented in Figure 1d. Inverted rectifying behavior was found in oxidized azurin (Figure S3).

The current-rectifying behavior of azurin is in agreement with its reported electrochemical behavior.[7−9,18] At $U_S = -0.3$ V, most of the molecules are in a reduced state, and efficient electron withdrawal from the $Cu^+$ center to a positively biased probe occurs (positive bias branch in Figure 1d; $U_{bias} = U_P - U_S$). At $U_S = 0.2$ V, azurin is oxidized, and the most efficient process is electron injection into the $Cu^{2+}$ center from a negatively biased probe[18] (Figure S3). From the $I-V$ characteristics, the conductance ($G$) of the tunneling gap in the presence of azurin was calculated from the relation $G = I/V$ to be between $10^{-6}G_0$ and $10^{-5}G_0$ (where $G_0 = 2e^2/h = 77$ $\mu$S is the quantum of conductance), in agreement with the reported azurin conductance.[10] Curves corresponding to clean Au(111) showed behavior consistent with a simple tunneling process, in which the $I-V$ curve can be described by the Simmons model and a linear dependence is expected at moderate biases (Figure S2).[21] In view of the $I-V$ characteristics in Figure 1c and Figure S3, we used reported procedures to identify a TV value that can be used to describe the electrochemical potential dependence of the azurin conductance in the context of TVS.[14] Briefly, we smoothed individual $I-V$ curves and plotted $\ln(I/V^2)$ versus $1/V$ (for further details, see the SI and Figure S4). The results are shown in Figure 2a and Figure S6c for reduced and oxidized azurin, respectively. Solid lines correspond to individual smoothed $I-V$ curves, and the dashed lines show the average of the $I-V$ curves for a bare gold sample for comparison. The azurin spectra displayed distributions of minima centered around 0.4 V, as shown by the histograms in Figure 2b and Figure S6d. No minima were found in the spectra of clean gold samples, although a TV would be expected for tunneling with the gold surface. We interpret this to indicate that the TV probably lies at a bias voltage outside the range of redox potentials of the working electrolyte. Similar results were obtained by an alternative approach in which $I-V$ plots were fit to the numerical version[22] of the Kuznetsov−Ulstrup (KU) two-step ET model[23] (see the discussion below and in the SI).

The TV found in the azurin spectra is the first one to be reported for a redox molecule in an electrochemical environment, and it is lower than the ones found for other single molecules.[12,14] It is on the same order as the TV reported for porphyrin dimers measured in air.[17] Although the calculation of a TV value for azurin is useful for the sake of comparison, it cannot be physically interpreted in the same terms as for small molecules confined between metal electrodes that undergo coherent electron transport.[12−14] Several ET studies of redox molecules have shown that a transition in conductance occurs when the application of an external potential results in the alignment of the molecular energy levels and the Fermi level of the electrodes.[24,25] Indeed, the low TV value obtained for azurin suggests that the effective barrier for tunneling through a solution is lower than the barrier found in pure tunneling processes (i.e., tunneling through vacuum), in agreement with experimental and theoretical works on tunneling through an electrochemical environment.[26−30] In particular, in the context of two-step ET in a redox molecule, a transition was predicted by theory to occur in the range where the effective voltage in the redox center is higher than the reorganization energy of the molecule.[25]

Considering the TV obtained experimentally as an expression of the shape of the energy barrier involved in the ET process in the system, we next sought to identify the main determinants of the TV in the conductance of a redox protein. For that purpose, we turned to the KU formalism for adiabatic two-step ET with partial vibrational relaxation,[25,31] which has been extensively applied to ECSTM experiments on azurin[8,32] and other redox molecules in electrochemical environments.[22] In the KU model, the current $I_T$ is given by eq 1:

$$I_T = e\kappa\rho(eU_{bias})\frac{\omega}{2\pi}\left\{\exp\left[\frac{e}{4\lambda kT}(\lambda + \xi\eta + \gamma U_{bias})^2\right] + \exp\left[\frac{e}{4\lambda kT}(\lambda + U_{bias} - \xi\eta - \gamma U_{bias})^2\right]\right\}^{-1} \quad (1)$$

in which $\kappa$ is the electronic transmission coefficient; $\rho$ is the density of states in the metal near the Fermi level; $\omega$ is the nuclear


dx.doi.org/10.1021/ja3080242 | J. Am. Chem. Soc. 2012, 134, 20218−20221

**Table 1. Average Values Obtained from Fits of the Experimental $I-V$ Curves to the Two-Step ET Model**

| configuration | Sample Potential $U_S$ (V/SSC) | Transition Voltage TV (V) | Reorganization energy $\lambda$ (eV) | Probe Coupling $\gamma$ | Substrate Coupling $\xi$ | Transmission Coefficient $\kappa$ |
|---|---|---|---|---|---|---|
| tunneling | −0.3 | 0.38 ± 0.18 | 0.56 ± 0.13 | 0.16 ± 0.04 | 0.74 ± 0.22 | 0.8 ± 0.3 |
| | 0.2 | −0.42 ± 0.08 | 0.60 ± 0.13 | 0.11 ± 0.02 | 0.75 ± 0.28 | 0.9 ± 0.2 |
| wired | 0.2 | −0.06 ± 0.01 | 0.90 ± 0.40 | 0.92 ± 0.15 | 0.64 ± 0.45 | 0.7 ± 0.4 |

vibration frequency; $k$ is Boltzmann's constant; $T$ is the temperature; $U_{bias} = U_P - U_S$ is the potential difference between probe and sample electrodes; $\lambda$ is the reorganization energy; $\eta$ is the overpotential, given by $\eta = U_S - U_{Az}$, where $U_{Az}$ is the redox potential of an azurin molecule; and $\gamma$ and $\xi$ are two model parameters describing the shifts in $U_{bias}$ and $\eta$ at the redox center, respectively. The parameters $\gamma$ and $\xi$ are related to the electronic coupling of the molecule with the probe and substrate, respectively.

To obtain values of the parameters for azurin, we fit the experimental $I-V$ curves to Pobelov and Wandlowski's numerical version of eq 1:[22]

$$I_T = 1820\kappa U_{bias}\left\{\exp\left[\frac{9.73}{\lambda}(\lambda + \xi\eta + \gamma U_{bias})^2\right] + \exp\left[\frac{9.73}{\lambda}(\lambda + U_{bias} - \xi\eta - \gamma U_{bias})^2\right]\right\}^{-1} \quad (2)$$

in which $I_T$ is expressed in nA, potentials are in V, and $\lambda$ is in eV. In this expression, typical values for $\omega$ in a liquid and $\rho$ in a metal were used,[22] and $\xi$, $\gamma$, $\lambda$, and $\gamma$ were left as free model parameters. An example of the fit of an $I-V$ curve is shown in Figure S5, and the resulting parameter values are summarized in Table 1.

Using eq 2 with the parameters in Table 1, we simulated $I_T$ numerically and plotted $\ln(I_T/V^2)$ versus $1/V$ (Figures S5 and S6). The resulting TVS plots displayed minima (corresponding to the TV) in the same range as our experimental spectra. We then examined how the TV depends on the different experimentally accessible parameters (overpotential, reorganization energy, and probe and surface couplings) and found that the coupling with the STM probe ($\gamma$) has the strongest impact. In particular, increasing the probe coupling from 0.1 to 1 reduced the TV almost 10-fold (from 0.44 to 0.05 V; Figure S7c).

With these simulations in mind, we examined TVS spectra corresponding to $I-V$ measurements on azurin in a wired configuration, where the STM probe is transiently bound to the protein[10] and recordings are made using the $I-t$ method[19] (Figure S8 and Table 1). Indeed, in ∼50% of the $I-V$ recordings, a minimum was found in the negative branch that corresponded to a very low TV (−0.06 ± 0.01 V), as predicted by the simulations. The variability of this measurement in wired junctions is consistent with the notion that the contact geometry dramatically affects the measured TV.[14,15,17] This minimum must be a reflection of the stronger coupling with the probe electrode, which lowers the energy barrier between the levels of the STM probe electrode and the molecule. Thus, in wired junctions, the TV is related to the contact resistance, as commonly found for single-molecule junctions.[14] Compared with thiol-bridged conjugated organic molecules, the ultralow TV value found for azurin may evidence better alignment of the protein redox level with the metal electrodes together with efficient electrical crosstalk between the azurin metal center and the electrodes of the junction. In the tunneling configuration, the TV is related to the tunneling barrier developed through the liquid gap between the molecule and the STM probe, as described by the distance decay factor $\beta \approx C \cdot TV^{1/2}$, with $C$ = 1.05 Å$^{-1}$ V$^{-1/2}$ .[14] This expression yields $\beta \approx 0.66$ Å$^{-1}$, in good agreement with the value we obtained for azurin under the same experimental conditions by current−distance electrochemical tunneling spectroscopy ($\beta$ = 0.5 ± 0.1 Å$^{-1}$).[18]

The coupling parameters $\xi$ and $\gamma$ reported in Table 1 agree with reported results[10] and are consistent with the conditions tested in each case: in tunneling experiments, the weak probe coupling indicates that an asymmetric junction is established, and the potential is dropped mainly at the protein−probe interface; in contrast, wired junctions are more symmetric and yield stronger probe coupling, with the voltage dropping mainly at the contacts. The reorganization energy is very similar to reported values.[8,10,32,33] Finally, the high values obtained for $\kappa$ indicate that ET occurs near the adiabatic limit and support the common assumption that $\kappa$ = 1.[22] However, this coefficient was obtained directly by fitting individual $I-V$ recordings and can be used to monitor deviations from adiabaticity.

Using the results described above, we built electrochemical energy diagrams for azurin in both the tunneling and wired

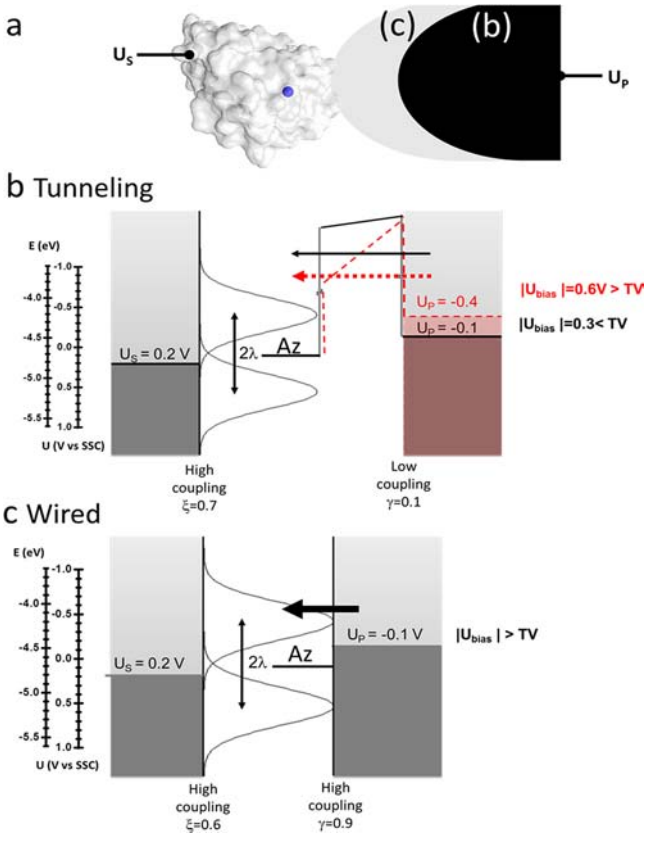


**Figure 3.** ET model. (a) Diagram of azurin between the surface and probe electrodes in the (b) tunneling and (c) wired configurations. (b) The effective tunneling barrier is lowered for $U_{bias}$ > TV (red diagram), resulting in a higher current than for at $U_{bias}$ < TV (black diagram). (c) In the wired configuration, azurin is strongly coupled to the probe, so the TV is low and the current is high at all values of $U_{bias}$.


dx.doi.org/10.1021/ja3080242 | J. Am. Chem. Soc. 2012, 134, 20218−20221

configurations as models to explain the ET between the protein and the electrodes. Figure 3a shows azurin chemically bound to the gold surface electrode, which is held at potential $U_S$. The ECSTM probe is held at $U_P$ at the tunneling distance (Figure 3b) or in contact with the protein in the wired configuration (Figure 3c). The energy diagrams correspond to the oxidized protein ($U_S$ = 0.2 V), but diagrams for the reduced state at $U_S$ = −0.3 V can be built in a similar way. In the tunneling configuration (Figure 3b), azurin is represented by its redox potential ($U_{Az}$ = 0.16 V)[32] and the parameters obtained above: $\lambda$ = 0.5 V, $\xi$ = 0.7 (strong substrate coupling), and $\gamma$ = 0.1 (weak probe coupling). At $U_P$ = −0.1 V, $|U_{bias}| = |U_P - U_S|$ = 0.3 V is below the TV obtained in this case (0.4 V), and the current is low (black diagram). At $U_P$ = −0.4 V, $|U_{bias}|$ is above the TV, and the current is higher through the effectively reduced barrier (red diagram). In the wired configuration (Figure 3c), the probe is strongly coupled to the protein ($\gamma$ = 0.9), and the low TV (0.06 V) gives rise to a high current at practically all values of $U_{bias}$.

In summary, we have reported the first $I-V$ measurements and TVS data for a redox protein under potentiostatic control. In the tunneling configuration, the azurin conductance revealed a transition with a TV value as low as 0.4 V, in agreement with recent studies of porphyrins in air.[17] The observed TV is consistent with previously measured distance decay factors for azurin in electrochemical environments.[18] The ultralow TV values obtained in the wired configuration show that electrode coupling is particularly optimized in the case of single-azurin junctions. Our measurements help in characterizing redox proteins and understanding their performance in biological ET chains and molecular electronic devices. Charge storage[34] occurs in the weak coupling configuration, and charge transfer is favored with strong coupling. From a biochemical perspective, these regimes are reminiscent of the two basic functions of azurin: to carry and exchange charge in ET chains. We have found that the TV is strongly regulated by the electronic coupling of the protein with the STM probe. In this study, azurin was immobilized, exposing the surface involved in the transient ET reactions with partner proteins under physiological conditions. Thus, these results suggest the intriguing possibility of gating between the two conductance regimes by varying the electronic coupling between the proteins, for example through the proximity of redox centers and protein−protein recognition.[35,36]

## ■ ASSOCIATED CONTENT

### Supporting Information

Experimental details and additional data. This material is available free of charge via the Internet at http://pubs.acs.org.

## ■ AUTHOR INFORMATION


### Corresponding Author

pau@icrea.cat

### Present Address

[⊥]Université de Nantes, BP 50609, 44306 Nantes, France.


### Notes

The authors declare no competing financial interest.

## ■ ACKNOWLEDGMENTS

This work was supported in part by Grants PET0808 and CTQ2008-06160 from the MICINN and 2009-SGR277 from the Generalitat de Catalunya. J.M.A. acknowledges a fellowship from the Generalitat de Catalunya (BE-DGR 2009). I.D.-P. thanks the Ramon y Cajal Program of the MICINN and the EU (International Reintegration Grant FP7-PEOPLE-2010-RG-277182) for financial support. The authors thank G. Gomila for helpful discussions.

## ■ REFERENCES


(1) Marcus, R. A.; Sutin, N. *Biochim. Biophys. Acta* **1985**, *811*, 265.
(2) Heller, A.; Feldman, B. *Acc. Chem. Res.* **2010**, *43*, 963.
(3) Lee, T.; Kim, S.-U.; Min, J.; Choi, J.-W. *Adv. Mater.* **2010**, *22*, 510.
(4) D'Amico, S.; Maruccio, G.; Visconti, P.; D'Amone, E.; Bramanti, A.; Cingolani, R.; Rinaldi, R. *IEE Proc.: Nanobiotechnol.* **2004**, *151*, 173.
(5) Willner, I.; Willner, B.; Katz, E. *Bioelectrochemistry* **2007**, *70*, 2.
(6) Sepunaru, L.; Pecht, I.; Sheves, M.; Cahen, D. *J. Am. Chem. Soc.* **2011**, *133*, 2421.
(7) Davis, J. J.; Wang, N.; Morgan, A.; Zhang, T.; Zhao, J. *Faraday Discuss.* **2006**, *131*, 167.
(8) Friis, E. P.; Andersen, J. E. T.; Kharkats, Y. I.; Kuznetsov, A. M.; Nichols, R. J.; Zhang, J. D.; Ulstrup, J. *Proc. Natl. Acad. Sci. U.S.A.* **1999**, *96*, 1379.
(9) Alessandrini, A.; Salerno, M.; Frabboni, S.; Facci, P. *Appl. Phys. Lett.* **2005**, *86*, No. 133902.
(10) Artés, J. M.; Díez-Pérez, I.; Gorostiza, P. *Nano Lett.* **2012**, *12*, 2679.
(11) Della Pia, E. A.; Elliott, M.; Jones, D. D.; Macdonald, J. E. *ACS Nano* **2012**, *6*, 355.
(12) Kim, B.; Choi, S. H.; Zhu, X. Y.; Frisbie, C. D. *J. Am. Chem. Soc.* **2011**, *133*, 19864.
(13) Beebe, J. M.; Kim, B.; Gadzuk, J. W.; Frisbie, C. D.; Kushmerick, J. G. *Phys. Rev. Lett.* **2006**, *97*, No. 026801.
(14) Guo, S.; Hihath, J.; Díez-Pérez, I.; Tao, N. *J. Am. Chem. Soc.* **2011**, *133*, 19189.
(15) Bâldea, I. *J. Am. Chem. Soc.* **2012**, *134*, 7958.
(16) Huisman, E. H.; Guédon, C. M.; van Wees, B. J.; van der Molen, S. J. *Nano Lett.* **2009**, *9*, 3909.
(17) Bennett, N.; Xu, G.; Esdaile, L. J.; Anderson, H. L.; Macdonald, J. E.; Elliott, M. *Small* **2010**, *6*, 2604.
(18) Artés, J. M.; Díez-Pérez, I.; Sanz, F.; Gorostiza, P. *ACS Nano* **2011**, *5*, 2060.
(19) Haiss, W.; Nichols, R. J.; van Zalinge, H.; Higgins, S. J.; Bethell, D.; Schiffrin, D. J. *Phys. Chem. Chem. Phys.* **2004**, *6*, 4330.
(20) Crane, B. R.; Di Bilio, A. J.; Winkler, J. R.; Gray, H. B. *J. Am. Chem. Soc.* **2001**, *123*, 11623.
(21) Simmons, J. G. *J. Appl. Phys.* **1963**, *34*, 1793.
(22) Pobelov, I. V.; Li, Z. H.; Wandlowski, T. *J. Am. Chem. Soc.* **2008**, *130*, 16045.
(23) Kuznetsov, A. M.; Ulstrup, J. *Electrochim. Acta* **2000**, *45*, 2339.
(24) Zhang, J. D.; Kuznetsov, A. M.; Medvedev, I. G.; Chi, Q. J.; Albrecht, T.; Jensen, P. S.; Ulstrup, J. *Chem. Rev.* **2008**, *108*, 2737.
(25) Zhang, J. D.; Kuznetsov, A. M.; Ulstrup, J. *J. Electroanal. Chem.* **2003**, *541*, 133.
(26) Pan, J.; Jing, T. W.; Lindsay, S. M. *J. Phys. Chem.* **1994**, *98*, 4205.
(27) Halbritter, J.; Repphun, G.; Vinzelberg, S.; Staikov, G.; Lorenz, W. J. *Electrochim. Acta* **1995**, *40*, 1385.
(28) Parsons, R. *Chem. Rev.* **1990**, *90*, 813.
(29) Nagy, G.; Wandlowski, T. *Langmuir* **2003**, *19*, 10271.
(30) Wigginton, N. S.; Rosso, K. M.; Stack, A. G.; Hochella, M. F. *J. Phys. Chem. C* **2009**, *113*, 2096.
(31) Kuznetsov, A. M.; Medvedev, I. G.; Ulstrup, J. *J. Chem. Phys.* **2007**, *127*, No. 104708.
(32) Alessandrini, A.; Corni, S.; Facci, P. *Phys. Chem. Chem. Phys.* **2006**, *8*, 4383.
(33) Chi, Q. J.; Farver, O.; Ulstrup, J. *Proc. Natl. Acad. Sci. U.S.A.* **2005**, *102*, 16203.
(34) Kim, S. U.; Yagati, A. K.; Min, J. H.; Choi, J. W. *Biomaterials* **2010**, *31*, 1293.
(35) Gray, H. B.; Winkler, J. R. *Q. Rev. Biophys.* **2003**, *36*, 341.
(36) Lyons, J. A.; Aragao, D.; Slattery, O.; Pisliakov, A. V.; Soulimane, T.; Caffrey, M. *Nature* **2012**, *487*, 514.